Regional Environmental Change manuscript No.
(will be inserted by the editor)

Inter-model variability of projected future wave-driven coastal sediment transport along the Catalan coast

Mercè Casas-Prat · Kathleen L. McInnes · Mark A. Hemer · Joan P. Sierra

Received: date / Accepted: date

Abstract In the context of climate change, this study evaluates the impact on the long-shore and cross-shore sediment transport (LST and CST) along the Catalan coast (NW Mediterranean Sea) derived from climate projections obtained from five combinations of regional and global circulation models (RCMs and GCMs). Special emphasis is given to how inter-model variability translates from wave projections to wave-driven coastal impacts, which is still poorly known. Results show that the uncertainty is in general larger, especially for LST, for which the discrepancies among regional models are more relevant than those associated to the forcing wave parameters. Such increase in the uncertainty can be explained by the nonlinear processes involved, and the role of the forcing wave parameters having sometimes competing effects (e.g. wave height vs. wave direction). This illustrates that the performance of each RCM-GCM can vary from forcing to impact parameters, hence, the suitability of a particular RCM-GCM to evaluate a certain impact should be assessed based on its ability to properly simulate such impact. In this regard, LST and CST rates computed using empirical formulae that integrate several wave climate parameters, as in this study, can be used as a non-computationally expen-

M. Casas-Prat*, J.P. Sierra
Laboratori d'Enginyeria Marítima, Universitat Politècnica de Catalunya · Barcelona Tech, Barcelona, Catalonia, Spain
Centre Internacional d'Investigació dels Recursos Costaners, Barcelona, Catalonia, Spain
*Now at Environment Canada, Science and Technology Branch, Climate Research Division, Toronto, Canada
E-mail: merce.casasprat@ec.gc.ca, joan.pau.sierra@upc.edu

K.L. McInnes
Centre for Marine and Atmospheric Research, CSIRO, Aspendale, Victoria, Australia
E-mail: Kathleen.Mcinnes@csiro.au

M.A. Hemer
Centre for Marine and Atmospheric Research, CSIRO, Hobart, Tasmania, Australia
E-mail: Mark.Hemer@csiro.au

sive tool to assess the suitability of a given RCM-GCM to project changes in coastal dynamics.

Keywords climate change · coastal sediment transport · wave climate · Mediterranean Sea

1 Introduction

Coastal areas are a focus for growing populations and economies (Nicholls and Kebede, 2012), in some cases already currently facing issues related to safety and/or recreational amenity. Many studies have provided increasing scientific evidence that ocean waves–one of the main drivers that shape our coastlines—are likely to be affected by a future warmer climate (e.g. Hemer et al, 2013). It is therefore important to assess the wave-driven coastal impacts potentially arising from climate change to design adaptation strategies to minimize the associated negative effects.

In the last decade, some studies have assessed the wave climate change impact on the coastal morphology for some regions. However, many of them are based on simplified wave climate change scenarios, which may not be realistic enough (e.g. Adams et al, 2011; Coelho et al, 2009; Dickson et al, 2009; Hemer, 2009). Some localised studies have explicitly accounted for the greenhouse effect—and some of their sources of uncertainty (e.g. Charles, 2012; Zacharioudaki and Reeve, 2011) but further research is needed to well-understand the regional variability of such coastal impacts.

The location of this study is the Catalan coast, situated in the NW Mediterranean Sea. The European EUROSION project (2002-2004, `http://www.eurosion.org/`, accessed January 2014) classified this coast, home of about three million people—40% of the Catalan population, as an area highly exposed to coastal erosion. Bosom and Jiménez (2011) found many stretches of the central Catalan coast being currently exposed to high levels of vulnerability to erosion. Indeed, during the last 50 years, erosion has been the dominant cause of reported damage along the Catalan coast (Jiménez et al, 2012). Acting on different time scales, long-shore and cross-shore sediment transport (LST and CST) are the main coastal processes that contribute to erosion. In this study we assess how these processes could change in a warmer climate due solely to variations in the wave climate. We do not consider other impacts driven by waves (e.g. coastal flooding, infrastructure damage, etc.) or other coastal drivers (e.g. sea level rise, storm surge, tides, etc.).

Casas-Prat and Sierra (2012) undertook a regional study along the Catalan coast based on extrapolated future wave climate obtained from the trend analysis of hindcast wave data of the second half of the last century. They identified important variations in the long-shore sediment transport, which amounted to a general reduction, but with high uncertainty. In this study we use wave projections that were forced by 10-m wind fields derived from the midline A1B scenario (IPCC, 2007) using five combinations of regional-global

climate models (Casas-Prat and Sierra, 2013). Note that the inter-model variability in surface wind speed, which drives the ocean surface waves, has been found to be one of the most important sources of uncertainty in climate change projections (Kjellström et al, 2011).

The contribution of this paper is twofold. First, it assesses the future impact of the greenhouse effect on wave-driven coastal sediment transport at the Catalan coast—as done for the first time in this area using climate projections that explicitly account for the rise in the greenhouse gas emissions. Second, towards a more general understanding of the range of climate change effects, this study provides insight into how inter-model climate variability translates from climate projections to coastal impacts, in this case, through changes in waves.

The rest of the paper is structured as follows. Section 2 provides a description of the datasets that are used. In Section 3 the methodology adopted to calculate the sediment transport is explained. Section 4 presents and examines the results and a final discussion is included in Section 5. Supplementary material is also provided to explain the main features of the study area in terms of both wave projections and geomorphological aspects.

2 Datasets

2.1 The forcing: wave climate

2.1.1 Wave projections

To project future long-shore and cross-shore sediment transport scenarios, this study utilizes 30-year regional wave climate projections at high temporal-spatial resolution (3 h and 0.125°). They were obtained by Casas-Prat and Sierra (2013) for the time slices: 1971-2000[1] (baseline period) vs. 2071–2100 (future period). Wave parameters were simulated with the SWAN model (Booij et al, 1999), which was forced by 5 wind climate projections, denoted as: HIR_E, RAC_E, REM_E, RCA_E and RCA_H. The first 3 characters of these acronyms stand for the regional circulation model (RCM) used whereas the last one is related to the driving global circulation model (GCM) (see Appendix A of supplementary material). Consequently, we involve a total of 4 RCMs driven by the same GCM and one RCM that is also driven by another GCM.

For winter and summer seasons (defined as December–January–February and June–July–August, respectively), Casas-Prat and Sierra (2013) analysed the present and the future mean and extreme wave climates from the median of the significant wave height (H_s) and the 50-year return period of H_s (z_{50}). The distribution of the mean wave direction (θ_m) and the types of sea states were also investigated. A summary of the climate change signals along the Catalan coast observed by Casas-Prat and Sierra (2013) that are relevant for

[1] 1981-2010 for REM_E model

LST and CST processes, is detailed in the supplementary material (Appendix A).

2.1.2 Wave hindcast

Additionally, we make use of the wave hindcast data of the HIPOCAS project (Guedes Soares et al, 2002). We calculate its associated LST and CST to compare with those obtained for the baseline period of the wave climate scenarios presented in Section 2.1. The HIPOCAS data set was obtained with the WAM model (Monbaliu, 2000) and forced by the wind output of the regional atmospheric model REMO (same RCM as for REM_E), which in turn was forced by the global re-analysis data of NCEP project (Kalnay et al, 1996). With a time resolution of 3 h, this dataset covers the period 1958–2001 but here we use only the last 30-year period (baseline period). Along the Catalan coast, the spatial resolution is 0.125° whereas it is 0.5° offshore. Similar to the majority of simulated data, HIPOCAS data tend to underestimate extreme events but the mean climate is well represented (Ratsimandresy et al, 2008). Casas-Prat and Sierra (2013) found that the median H_s field obtained with HIPOCAS is similar to that of RCA_E and RCA_H (see Section 2.1.1).

2.2 The receptor: beaches

The sediment transport depends not only on the forcing wave climate but also on the beach geomorphology (eg. van Rijn et al, 2003) The Catalan coast, with a length of about 780 km, encompasses a large geo-diversity of coastal types such as cliffs, bays, pocket beaches, long straight beaches and deltas (Jiménez et al, 2012). In this study we are assessing the impact of wave climate change on the LST and CST, that principally affect sandy beaches. In the supplementary material, a brief description of the main regional features is included (Appendix B).

The parameters that characterize the beach and will be used in the LST and CST computations are (see Section 3): the mean beach slope ($\tan\beta$), the median of the sediment grain size distribution (d_{50}) and the mean beach orientation (γ) (see Figure SM3 of supplementary material). For the Catalan coast this information was acquired during beach profiling and sediment sampling field campaigns (CIIRC, 2010).

In this study we assume that current values of $\tan\beta$, d_{50} and γ will remain valid into the future. This entails a limitation in the analysis because natural beaches gradually tend to re-adapt to changing wave conditions and they also might evolve forced by other drivers (e.g. sea level rise). However, major (long-term) changes in $\tan\beta$, d_{50} and γ are expected to be limited since the majority of the Catalan beaches are significantly engineered and/or human-controlled.

3 Methodology

As mentioned in the Introduction, the effect of the sediment transport is separately assessed by means of the long-shore and cross-shore components, which usually act at different time scales and are controlled by different wave regimes. Long-shore sediment transport (LST) is modulated by the mean wave climate in a seasonal to decadal time frame. On the contrary, cross-shore sediment transport (CST) tends to occur at a shorter time scale. In this study, we only consider the beach erosion due to CST, which is an hourly to weekly process controlled by the extreme wave climate. The beach recovery that occur between storms is not assessed.

Two widely used approaches to estimate the sediment transport are: (i) bulk transport formulas and (ii) process based models. The former are commonly used in management or engineering applications and are based on simplified representation of pysical processes which use empirical coefficients. The latter are more detailed and include a large number of physical processes but need a large number of input parameters which need to be calibrated per application (Mil-Homens et al, 2013). In this study, we use the first type of empirical (physical-based) approach (ie. i) to compute both LST and CST (see Sections 3.1 and 3.2, respectively). With this approach, we can easily obtain a regional picture of the potential coastal impacts and evaluate their sensitivity to changes in the wave climate without significant computational cost. These empirical methods have certainly some limitations though. For example, despite reproducing a similar spatial pattern, CIIRC (2010)'s study showed that the choice of the LST formula can induce deviations of a factors 10. However, they did not apply the formula used in this study (see Section 3.1), which is recommended by Leont'yev (2014), as long as the size of the sediment does not change significantly along the profile. Anyway, the analysis of the results (Section 4) will not focus on the accuracy of punctual values but in the spatial performance, which can be properly assessed if the same methodology is consistently applied all along the coast.

Recently some studies (Callaghan et al, 2013; Wu and Dong , 2015) have also accounted for the stochastic nature of the shoreline evolution by means of using a probabilistic approach. In the present study, however, we focus on the inter-model variability and we use a deterministic approach to compute LST and CST.

3.1 Long-shore sediment transport (LST)

As waves approach the coast, they break and generate a long-shore current which moves beach material parallel to the coast within the surf-zone. To estimate this transport we use the well-known CERC formula (see Eq.1) in which LST is proportional to the long-shore wave energy flux.

$$Q = \frac{K\rho}{16(\rho_s - \rho)(1-a)} H_{s,b}^2 C_{g,b} \sin(2\alpha_b) \tag{1}$$

where Q is the LST produced by the wave conditions at breaking defined by: the significant wave height ($H_{s,b}$), the group velocity ($C_{g,b}$) and the angle between the the coastline (α_b) and the wave crest (perpendicular to the wave direction θ_m) and the coastline (α_b). ρ is the density of water ($\rho = 1026$ kg/m^3), ρ_s is the density of sand ($\rho_s = 2650$ kg/m^3) and a is the porosity index ($a = 0.4$). As in the study of Casas-Prat and Sierra (2012), K is estimated in terms of wave and sediment properties, with the formula of Bayram et al (2007), which, as mentioned before, has been recommended by Leont'yev (2014):

$$K = \frac{135}{256}\frac{\gamma_b \pi}{c_\mathrm{f}}\varepsilon\,; \quad \varepsilon = \left(9 + 4\frac{H_{s,b}}{\mathrm{w}_s T_p}\right)10^{-5} \tag{2}$$

where c_f is the friction coefficient ($c_\mathrm{f} = 0.005$), γ_b the breaking index ($\gamma_b = 0.78$), w_s the sediment settlement velocity, T_p the peak wave period and ε the portion of wave energy effective to move the sediment. w_s is estimated in terms of d_{50} using the formula of Jiménez and Madsen (2003). Mil-Homens et al (2013) proposed an improved Bayram formula but we prefer to use the original formula of Bayram et al (2007) because Mil-Homens's proposed coefficient does not depend on the sediment properties. This could be explained by the fact that they used a dataset with 94% of the data points having D_{50} smaller than 0.5 mm, which is not the case of the present study (see the D_{50} distribution along the Catalan coast in Figure SM3). In addition, Mil-Homens et al (2013) showed that, contrary to other formulations, the original formula of Bayram et al (2007) already presented a small bias.

For each beach n, $n = 1, ..., N$ (N the total number of beaches, N=299 in this study), the corresponding offshore forcing wave conditions are extracted from the wave projections described in Section 2, considering the nearest wave grid point m_0 from those plotted in Figure 1. Particularly, we use the following wave parameters (at deep water): significant wave height $H_{s,0}$, mean wave direction $\theta_{s,0}$ and peak wave period $T_{p,0}$. To obtain the conditions at breaking, we use the linear wave propagation (Snell's law) taking into account the refraction and shoaling processes and assuming a constant peak wave period ($T_{p,b} = T_{p,0}$). Instead of propagating every single value of the 30-year 3-hourly wave time series $\{H_{s,0}, \theta_{s,0}, T_{p,0}\}$ of each present/future time period obtained by each climate model, only a set of representative wave conditions are propagated and used to compute LST. Specifically, we divide the wave data into k groups: 8 directional sectors $\Delta\theta_i$, $i = 1, ..., k_\theta$ ($k_\theta = 8$), of 45° each (N, NE, E, SE, S, SW, W, NW) and 5 groups of H_s, ΔH_i, $j = 1, ..., k_H$ ($k_H = 5$, [0–1, 1–2, 2–3, 3–4, >4] m). Therefore, $k = k_\theta \cdot k_H = 40$. The LST associated with each group ($Q_{\Delta H_j, \Delta\theta_i}$), is then computed using the following representative values: $H^R_{s,0}$ =[0.5, 1.5, 2.5, 3.5, 5] m, $\theta^R_{m,0}$=[0, 45, 90, 135, 180, 225, 270, 315]°(in this study we use the Nautical convention for θ). The corresponding $T^R_{p,0}$ are obtained after averaging all period values for each group $\{\Delta H_j, \Delta\theta_i\}$ (R stands for "representative"). As shown in Eq. 3, the annual (net) LST (Q_annual) is finally obtained as the addition of all $Q_{\Delta H_j, \Delta\theta_i}$ values with the corresponding sign (positive from north to south, and viceversa). Also, they

are respectively weighted by the frequency of occurrence of each wave group $\{\Delta H_j, \Delta\theta_i\}$ (calculated for each wave climate projection and time period).

$$Q_{\text{annual}}(n) = \sum_{i=k_{\theta_1}(n)}^{k_{\theta_2}(n)} \sum_{j=1}^{k_H} Q_{\Delta H_j,\Delta\theta_i}(n) \cdot f_{\Delta H_j,\Delta\theta_i}(m_0(n)) \tag{3}$$

Note that $i = k_{\theta_1}(n), ..., k_{\theta_2}(n)$ in Eq. 3, rather than $i = 1, ..., k_\theta$. This is to account only for the range of wave directions $[\theta_1, \theta_2]$ that are effective to generate LST for a certain beach n. In this regard, k_{θ_1} and k_{θ_2} are obtained taking into account the beach orientation (γ) together with the nearby obstacles, such as coastal infrastructure or natural promontories. Additionally, a filter is added to LST computation—for beaches shorter than 1 km, directly $Q_{\text{annual}} = 0$ since waves need a certain distance to generate significant LST rates.

3.2 Cross-shore sediment transport (CST)

At event or seasonal time scale, erosion/accretion can also occur due to CST, which governs the short term beach dynamics and encompasses both offshore and onshore transport. In this study, the effect on the CST is estimated by means of the beach erosion potential defined by Mendoza and Jiménez (2006) in terms of the eroded volume V. Using the beach profile evolution model SBEACH (Larson and Kraus, 1989), they obtained Eq. 4 to calculate V (in m^3/m) of a certain beach profile with slope $\tan\beta$, caused by the impact of a wave storm with mean significant wave height $H_{s,0}$, mean peak period T_p and storm duration τ. Storms are defined with the peak over threshold method considering $H_s > 2$ m and $\tau > 6$ h with additional duration requirements in order to select independent storms (Mendoza and Jiménez, 2006). Also, only those storms with a mean θ_m within the range of effective wave directions $[\theta_1, \theta_2]$ (as for LST computation, see Section 3.1) are considered.

$$V = 4.5[(D_0 - D_{0,e})^{0.5}\tau \tan\beta] + 5.02, \quad \text{for } D_0 > D_{0,e} \tag{4}$$

where D_0 is the Dean parameter for deep water:

$$D_0 = \frac{H_{s,0}}{\text{w}_s T_p} \tag{5}$$

and $D_{0,e}$ is D_0 at equilibrium ($D_{0,e} = 2.7$). As for LST computation, the deep water wave parameters are obtained using the wave grid points plotted in Figure 1 and w_s is estimated in terms of d_{50} using the formula of Jiménez and Madsen (2003).

For both the baseline and the future periods (and each model configuration), a time series of $\{V\}$ is therefore obtained with Eq. 4. Afterwards, the (temporal) median of V and the cumulative value over the 30 years (V_{cum})

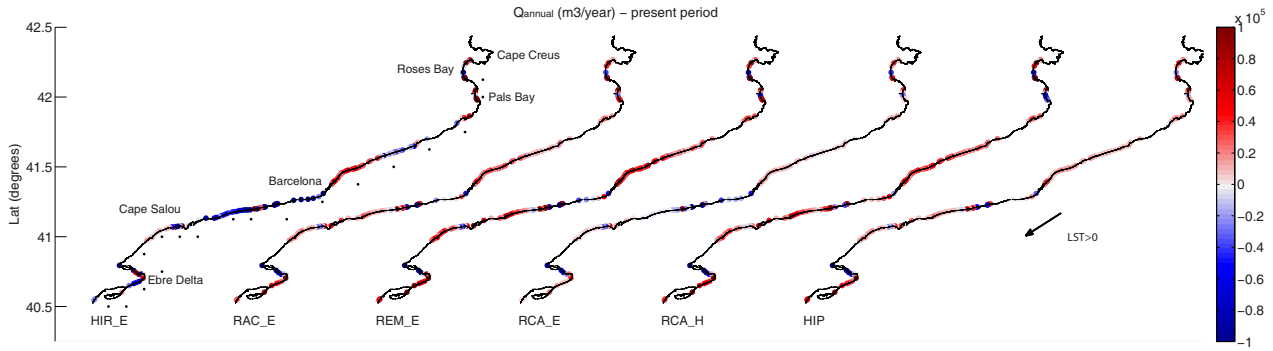

Fig. 1 LST (in m^3/year) for the baseline period corresponding to the 5 RCM-GCM models and HIPOCAS data (HIP). The first coastline plot indicates some relevant locations, as well as the offshore grid points used to derive the forcing wave conditions.

associated with each simulation is used to analyse and compare the CST results. The first parameter gives an idea of the average erosion given a storm episode. V_{cum} is the total volume of sediment lost over the 30 years and it is related to the rate of sediment exchange. During mild wave conditions, the beach would gradually restort the pre-storm beach profile. However, if severe erosion events are very frequent (which translates into a high V_{cum}), the beach might not be able to recover completely. As mentioned before, the recovery between storms due to on-shore sediment transport has not be taken into account in this study. Therefore V_{cum} is not a real accumulated erosion but it indicates the total sediment lost in a 30-year time period that needs to be recovered between storms to be in equilibrium.

4 Results

In this section, results of LST and CST are presented and related to the driving wave climate changes, mostly to those occurring in the winter season. In spite of LST being estimated for the whole year, the most energetic winter waves are the ones that mostly contribute to the annual LST. Additionally, CST is controlled by the most extreme waves, which usually occur during winter.

With special focus on the inter-model variability, for both LST and CST, the performance for the baseline period is assessed, first, and, afterwards, the climate change signals are examined.

4.1 Long-shore sediment transport (LST)

4.1.1 Baseline period

Figure 1 illustrates the LST results for the present (baseline) period associated with the 5 combinations of RCM-GCM and HIPOCAS data (see Section 2.1).

Positive values (red colour) denote LST going from north to south (see arrow in Figure 1), whereas negative values (in blue) indicate the opposite result. Except for HIR_E, the (spatial) 90 percentile of Q_{annual} is below 100,000 m^3/year, which is a reasonable value for this area. Median (absolute) values range from 7,000 m^3/year (RCA_E) to 38,000 m^3/year (HIR_E and REM_E). The spatial pattern of HIPOCAS-driven LST is similar to that of RAC_E, REM_E and RCA_H but with lower intensity.

Except for HIR_E (and RCA_E to some extent), all models reproduce a general positive LST, which is in agreement with current observations (CIIRC, 2010). Zonally, they also correctly reproduce the existing LST spatial pattern at the Ebre Delta, which is one of the factors that explains the current delta's beach retreat (see Appendix B of supplementary material): negative(positive) LST rates north(south) of the river mouth (CIIRC, 2010). The Ebre delta, which river mouth is roughly located at the most eastward point, is mainly affected by marine erosional process since the Ebre river is highly regulated by dams which notably limits the sediment transport along the river (e.g. Vericat and Batalla , 2006). Also, the negative LST in some beaches south of Cape Salou that are sheltered from NE waves is well-captured. However, LST results are in general not very accurate (neither using HIPOCAS data) where the orography is very irregular like south of Cape Creus. The reason might be related to the LST computation and, more specifically, to the linear wave propagation. Even though the shadowing effect of obstacles like Cape Creus is introduced with the range of effective wave directions (see Section 3.1), neither the actual bathymetry is accounted for, nor complex wave propagation processes such as wave diffraction.

Given the unrealistic LST spatial pattern obtained with HIR_E for the baseline period, the associated RCM-GCM combination is considered not to be suitable to evaluate the future LST in the study area. With respect to the wave climate, HIR_E already stood out from the other simulations as pointed out by Casas-Prat and Sierra (2013). However, the discrepancies in terms of Q_{annual} are higher than in terms of the analysed wave parameters (for example, major discrepancies were not obtained in terms of the wave direction frequency distribution, see Casas-Prat and Sierra (2013)).

Compared to other simulations, lower (absolute) values of Q_{annual} are obtained for RCA_E (especially for the positive range). This is in agreement with the lower median H_s obtained using this climate model configuration, that seems to be caused by the spatial-averaged forcing wind fields associated with this RCM (Casas-Prat and Sierra, 2013). However, the RCA_H-driven wave climate, which produced even lower values of the median H_s due to being forced by the same RCM as RCA_E, has LST rates similar to RAC_E and REM_E (Figure 1). The reason for this result seems to be related to the differences in θ_m induced by the different driving GCMs: ECHAM5 for RCA_E and HadCM3Q3 for RCA_H. In particular, there is a larger fraction of waves coming from the east sector for RCA_H-driven wave climate, which generally contributes to a positive LST along the Catalan coast (see Appendix A of supplementary material).

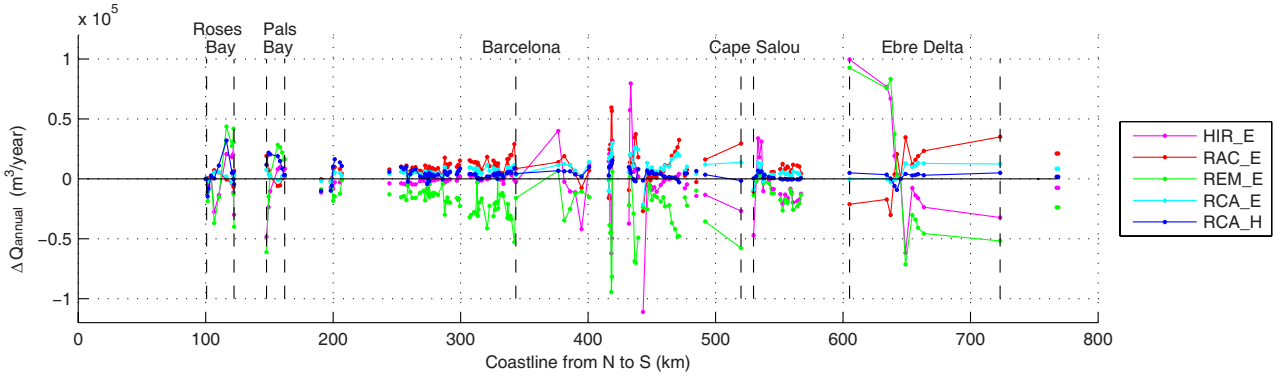

Fig. 2 Projected absolute change in LST (in m^3/year) for the 5 RCM-GCM models. The locations indicated in Figure 1 are also shown.

4.1.2 Climate change signals

Figure 2 illustrates the projected LST changes (difference between the future and the present Q_{annual}) along the Catalan coast associated with each climate model. The location of each beach is plotted as a function of the distance along the coastline from the northernmost side, projected onto the x-axis. More than 90% of the locations predict a change in Q_{annual} below 30,000 m^3/year. With local exceptions, this change is positive for RAC_E, RCA_E and RCA_H, and negative for REM_E. Their spatial median relative changes are, respectively: 42%, 43%, 7% and -47%.

The increase of Q_{annual} associated with RCA_H (dark blue line) was expected taking into account the general increase of the frequency of E waves (see Figure SM2 of supplementary material), which contribute to generate a positive LST. However, it is surprising to see how results corresponding to different RCMs but the same GCM (RAC_E, RCA_E vs. REM_E—red and cyan lines vs green line) have such a different response in terms of LST even though their projected mean wave climate change signal was similar (see Figure SM1 of supplementary material). Indeed, Q_{annual} changes associated with RCA_E are surprisingly close to those of RCA_H despite the large differences in the climate change signals of the corresponding wave direction field.

RAC_E, RCA_E and REM_E all project for winter more waves in the S-SW sector accompanied by fewer waves from the NE-E one (see Figure SM2 of supplementary material). Superficially, this would seem to suggest a decrease in the LST component, as obtained just for the REM_E case. Here it is worth pointing out that the tendency of Q_{annual} to decrease was also obtained by Casas-Prat and Sierra (2012) (see Introduction) when performing a trend analysis with the HIPOCAS data, which uses the same regional model as REM_E (although driven by different global data) (see Section 2.1.2).

To better understand LST changes, we need to get deep insight into the wave climate signals. On the one hand, we observe that predicted changes

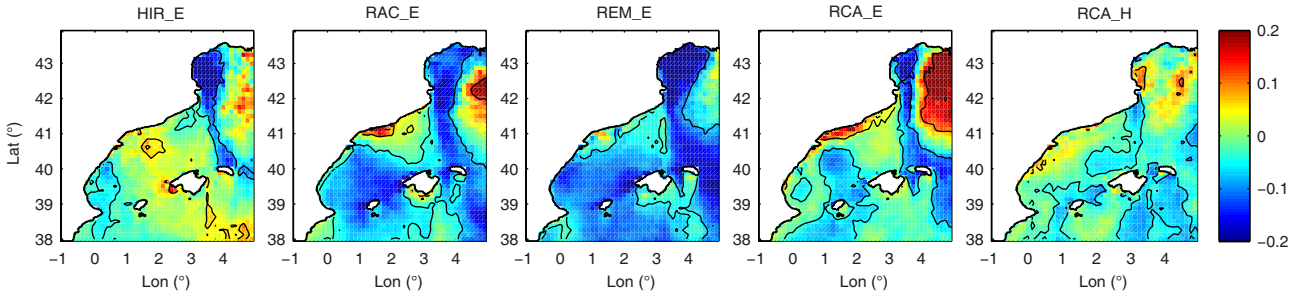

Fig. 3 Projected relative change in the mean H_s (-) for waves coming from NE during winter, for the 5 RCM-GCM models

in the frequency of θ_m and the intensity of H_s for a given direction lead sometimes to competing effects, as similarly found out by Charles (2012). For instance, Figure 3 illustrates the relative change of the mean H_s during winter just for those waves coming from NE. Close to the Catalan coast, these waves are expected to be higher for RAC_E and RCA_E simulations, which may counteract the effect of having less waves coming from that direction (see Figure SM3 of supplementary material) and therefore producing an increase in Q_{annual} for RAC_E and RCA_E, rather than a decrease. On the other hand, the high uncertainty of the extreme wave climate projections (see Figure SM1 of supplementary material) might give rise to Q_{annual} inter-model variability despite LST being a process mainly dominated by the mean wave climate. For example, z_{50} associated with REM_E suffers from a notably more accentuated reduction than the other models, which further contributes to the Q_{annual} reduction associated with REM_E.

Clearly, the inter-model variability is accentuated in terms of Q_{annual}, if compared with that of the wave climate, especially the mean wave climate. For some areas, this variability can lead to important differences in the tendencies of erosion/accretion. At the Ebre delta, for example, REM_E projects an increase(decrease) north(south) of the river mouth whereas RAC_E predicts the opposite. Taking into account the present LST pattern, the later response would lead to an increasing rate of the delta's beach retreat.

4.2 Cross-shore sediment transport (CST)

4.2.1 Baseline period

Figure 4 shows the results of both the median of V (top) and V_{cum} (bottom) for the baseline period. Compared to Q_{annual}, the inter-model variability is lower (especially for the median V): the spatial pattern is more or less consistent among models (although with different magnitudes). The factors that seem to contribute to enlarge this agreement are the following. First, θ_m—that has a large degree of uncertainty in the context of climate projections, is not

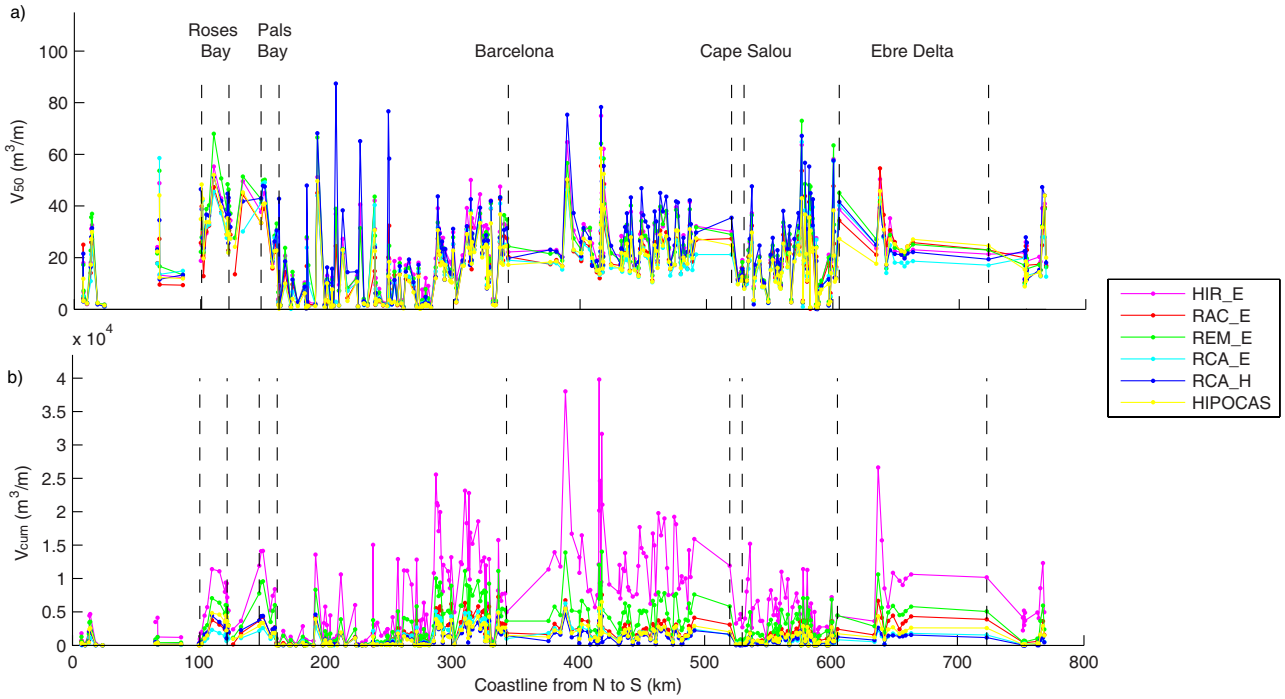

Fig. 4 Simulated V (m^3/m) for the baseline period for the 5 RCM-GCM models and HIPOCAS data. (a) Median of V.(b) Cumulative V

considered in CST computation (whereas it plays an important role for LST). Second, the fact of including the ratio between H_s and T_p—variables with a close relationship for wind-sea states—contributes to reduce the effect of model biases because they are highly correlated in this area due to the short fetches (Casas-Prat and Sierra, 2013).

The (temporal) median of V has a spatial median between 16 m^3/m and 21 m^3/m and the 90 percentiles are between 32 m^3/m and 43 m^3/m. The larger extreme values of the median of V are achieved by RCA_H. Paradoxically, this RCM-GCM configuration simulates relatively low(high) median values of $H_s(T_p)$ for stormy conditions (not shown) but their storms are on average longer, which highlights the strong dependence of V on τ. Results associated with REM_E exhibit the second largest extreme values of the median of V (first ranking in the northern part of the coast), thanks to a combination of relatively high(low) values of H_s and $\tau(T_p)$ (for stormy conditions). HIPOCAS results show, in general, a low value of V (especially for extremes), having similar values to RAC_E and RCA_E. The similarity with these two models is more or less maintained in terms of H_s, τ and the number of storms but not for T_p (it is significantly larger for HIPOCAS). For example, the spatial median of T_p is 8.4 s for HIPOCAS whereas ranges from 7.7 s to 8.0 s for all the other models. Apart from having a different atmospheric forcing, which influences

this result, the disparity in terms of T_p particularly, can be related to the wave model used. As explained in Section 3, HIPOCAS was obtained with WAM, whereas the remaining wave projections were simulated with SWAN. Bolaños-Sanchez et al (2007) already found some discrepancies between these two wave models in terms of T_p (using the same forcing) and the recent study of Pallarès et al (2014) has pointed out that, for the study area, SWAN tends to underestimate T_p (comparing simulations with measurements).

As aforementioned, the cumulative value (V_{cum}) shows a larger inter-model variability. This is the result of this parameter being largely affected by the number of storms, which exhibit a larger variability among models (especially between HIR_E and the rest). HIR_E clearly shows the larger values of V_{cum} because, apart from larger values of H_s for stormy conditions (not shown), it simulates a greater number of storms (in many locations, more than double of that of the other models). This result suggests that this model overestimates the cumulative erosion potential too. The second largest values of V_{cum} are obtained for REM_E, that combines high values of τ and the number of storms (not shown).

Another interesting conclusion can be yielded from these results: spatial variability is largely affected by morphological features and that might also explain the larger consistency of the spatial patterns among models. The two geomorphological parameters explicitly included in CST computation, Eq. 4, are $\tan\beta$ and d_{50} and they are usually related: steeper beaches normally have coarser sediment and viceversa. Mendoza and Jiménez (2006) showed that, for the same storm, reflective beaches ($d_{50} >= 0.6$ mm and $\tan\beta \sim 0.1$) had a larger erosion potential than dissipative beaches ($d_{50} \sim 0.25$ mm and $\tan\beta \sim 0.01$). On average terms, our results follow this tendency but this pattern is not always maintained as explained by Eq. 4. According to this equation, higher values of $\tan\beta$ are associated with a greater erosion potential but d_{50} induces the opposite effect. Additionally—and this is an important limiting factor, for a given storm s, there is a maximum grain size that can be mobilized (say $d_{50}^{\mathrm{max.}}(s)$) independently of the value of $\tan\beta$ (in order to fulfil $D_0 > D_{0,e}$). This is reflected in the fact that, for example, beaches north of Barcelona—typically reflective, achieve both very low and very high values of the median of V (Figure 4). The first case occurs for beaches with a very coarse sand for which $d_{50} > d_{50}^{\mathrm{max.}}(s)$ for many storms s. For beaches with finer sand, the threshold condition $D_0 > D_{0,e}$ is fulfilled more often, enabling the role of $\tan\beta$. Actually, regressing $\tan\beta$ against the median of V (not shown), we could see that high values of erosion potential are necessarily associated with relatively steep beaches but not the other way around (steep beaches can have a low erosion potential).

Moreover, the coastal orography plays an important role through the range of effective wave directions (see Section 3.1). For example, despite the most energetic waves typically threatening the northern Catalan coast, comparatively low values of V_{cum} are obtained along this coastal stretch because the rugged coastline offers shelter from high waves coming from many directions, reducing the number of storms capable to erode the beach.

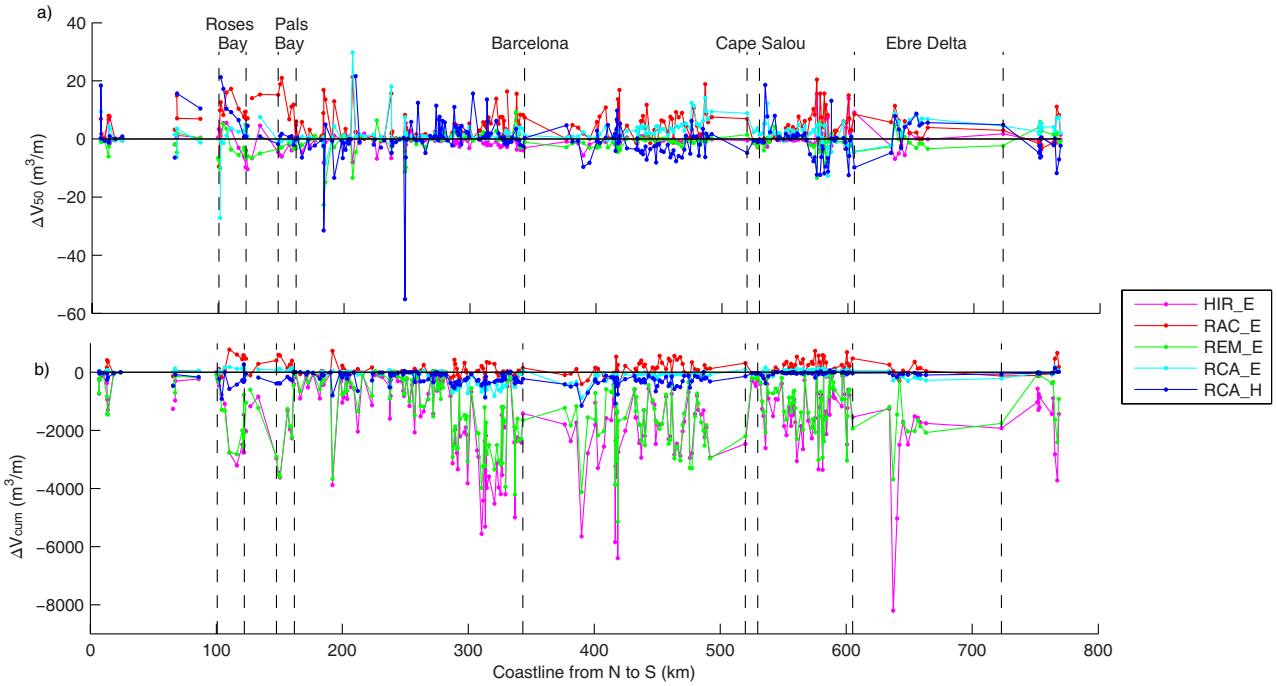

Fig. 5 Projected change of V (m^3/m) for the baseline period for the 5 RCM-GCM models. (a) Median of V.(b) Cumulative V

4.2.2 Climate change signals

Figure 5 shows the projected future changes for both the median of V (top) and V_{cum} (bottom). To better understand the climate change signals, Figure 6 illustrates the changes (difference between the future and the present period) found for the driving (stormy) wave conditions (from top to bottom): the median of H_s, T_p and τ and the number of storms (# storms).

Along the coastline, most of the simulations oscillate between positive and negative changes for the median of V (especially for HIR_E, REM_E and RCA_H) whereas there is a common tendency for V_{cum} to decrease (except for RCA_E). In terms of the (temporal) median of V, the spatial median is positive only for RAC_E (18%) and RCA_E (11%) but close to zero for RCA_H. Coastal areas showing a more or less consistent positive change for more than two RCM-GCM combinations are the central part of the coast north of Barcelona and the mid-southern part of the Ebre delta, which could enhance the current problems of beach retreat. Simulations driven by RAC_E show the largest percentage of beaches for which the erosion potential rises for both the median of V and V_{cum}. This can be explained by the fact that this model configuration projects the largest increase in terms of H_s and τ (Figure 6), the latter representing a spatial median relative change of 23% (whereas the other

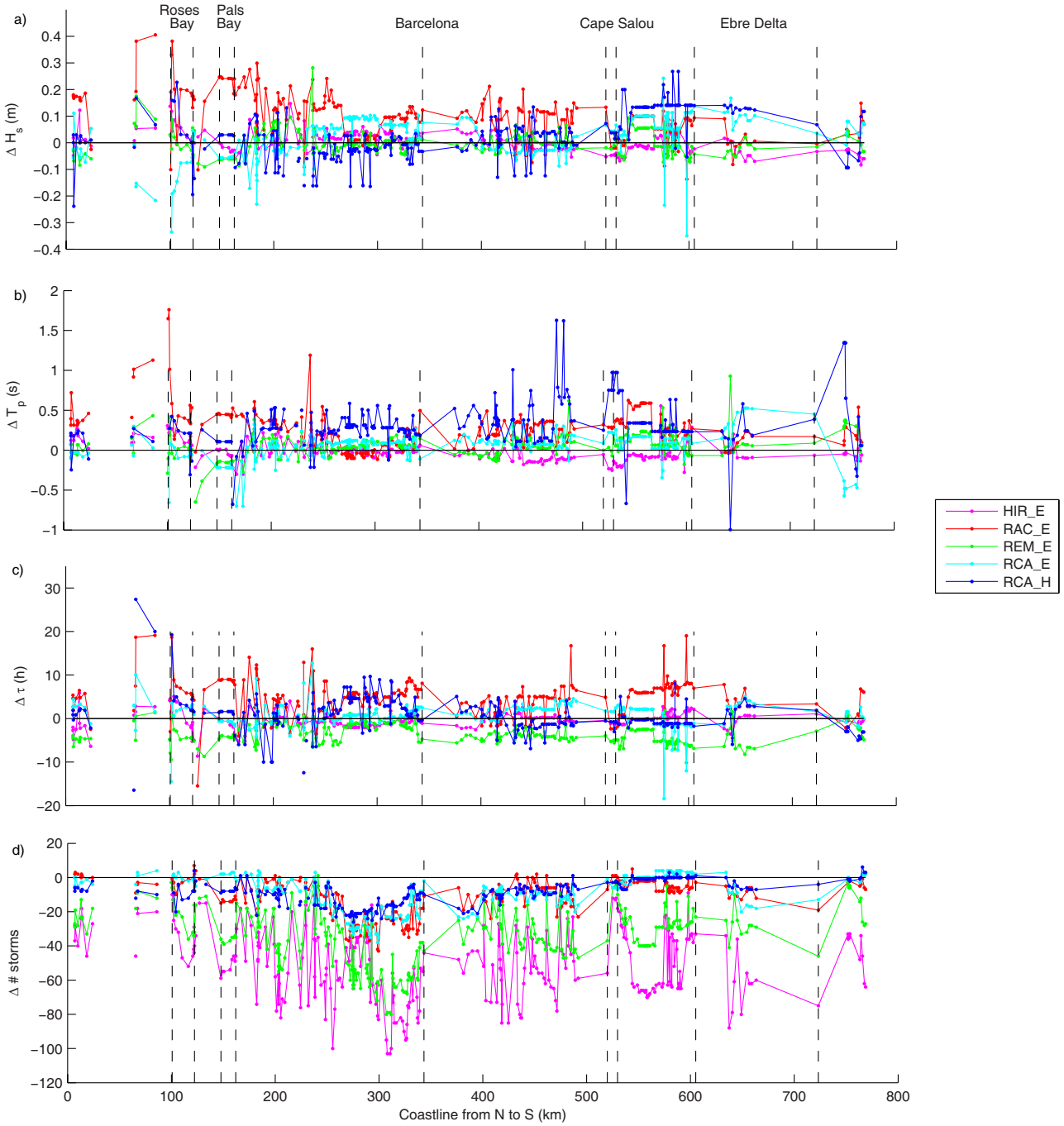

Fig. 6 Projected change for the 5 RCM-GCM models in: (a) the median of H_s, (b) the median of T_p, (c) the median of τ and (d) the number of storms. All these parameters are relative to the storms with effective wave direction

two positive values are for RCA_E and RCA_H which amount to 4% and 1%, respectively).

As aforementioned, V_{cum} has a general tendency to decrease (except for RAC_E) but this reduction is accentuated for HIR_E and REM_E (Figure 5) with a spatial relative decrease of 24% and 38%, respectively. For HIR_E results, this can be mainly explained by a large reduction in the number of storms (spatial median relative change of -23%) and, for REM_E, by both a reduction in the number of storms and τ (spatial median values of -29% and -13% respectively). All models present, indeed, a general decrease in the number of storms, with a median relative reduction of at least 11%. The tendency to decrease is observed not only for the effective number of storms (Figure 6) but also for the total number of storms (not shown), which is consistent with the reported decrease in the number of cyclones in the Mediterranean (Christensen et al, 2007). Actually, a negative trend in the number of storms has already been observed in the Ebre delta between 1990 and 2006 using measured wave data (Sánchez-Arcilla et al, 2011).

The pattern of change of H_s and T_p exhibit some discrepancies, consistent with the uncertainty stated in Christensen et al (2007) about whether or not the cyclones in the Mediterranean will be more intense in the future. Inter-comparing H_s and T_p, we confirm the different behaviour of RCA_H (see Section 2.1.1), showing a notable tendency of T_p to increase whereas H_s moderately increases or even decreases. This is reflected in the spatial median of the relative change: 3.4% for T_s whereas 0.7% for H_s. This is in agreement with the fact that this model project a larger influence of swell waves, as explained in Appendix A of supplementary material. Despite H_s and T_p changes poorly contributing to enhance V in RCA_H case, in some locations (central coast north of Barcelona or Ebre delta)) an increase of the median of V is found for this simulation. This can be explained by the rise of τ, pointing out the important role of this storm parameter for the erosion potential, as mentioned in Section 4.2.1.

5 General discussion

Coastlines respond to both mean and extreme wave climate characteristics and so assessing future changes must also consider the changes to both means and extremes. However, the representation of extreme climate characteristics is typically not well described by GCMs due to the limited spatial and temporal resolution of the models. Therefore, higher resolution climate models simulations are usually downscaled using RCMs. As shown in this study, RCMs however add significant uncertainty in the coastal sediment transport responses.

Casas-Prat and Sierra (2013) pointed out that discrepancies in the wind projections could be enhanced in terms of the wave climate due to the non-linear relationship governing the wind-sea states and the favouring character of certain fetch conditions. Nevertheless, except for winter wave extremes, a

large amount of the inter-model variability could be explained by GCMs. This study shows how the downscaling procedure from the regional wave climate to the local coastal dynamics further accentuates climate model biases and their inter-model variability, especially for LST, for which wave direction plays an important role. This result highlights that the local-regional scale response of coastline to the broader scale changes in climate is a challenging problem.

The rise in the uncertainty can be partly explained by the non-linear relationship governing the sediment transport processes, that can exaggerate the discrepancies present in the wave driving factors. Also, the problem is further complicated because not only one but a set of wave parameters have an important role in coastal dynamics. For example, as observed by Charles (2012) in the LST changes along the Aquitanian coast (France), this study shows that for the Catalan coast as well, the expected changes in wave height and wave direction can lead to opposite changes in LST. This complexity makes difficult to predict beforehand the resulting net effect. In terms of CST, the general effect of the reduction in storms, which alone would be expected to reduce CST, can be countered by increased storm duration.

In spite of the uncertainty, we think that this study's results can serve as a guideline to locate and design further local assessment studies (e.g. beach retreat at the Ebre delta) that can afford the use of more accurate but computationally more expensive morphodynamic numerical models, like in the studies of He et al (2015) and Villaret et al (2013), who used DELFT3D and TELEMAC, respectively. The latter approach can give a better estimation of the present and future sediment transport rates and changes in the beach configuration, although they will still be affected by the variability in the driving wave projections. In this respect, further research is needed to try to reduce the variability in the future (forcing) projections.

Finally, we think that if looking at the problem from a different perspective, LST and CST projections can bring additional value towards the assessment of the underlying RCMs and GCMs. Many studies have pointed out that the capability of climate models to properly reproduce the (atmospheric) climate system depends on the output variable or the physical aspect under evaluation (e.g. Kjellström et al, 2011). This is one of the reasons why it is, in general, so difficult to choose a "top" sub-set of climate models. Moreover, considering how uncertainty propagates to coastal impact parameters as shown in this study, it would be risky to establish a set of "best" climate models only based on their atmospheric or wave climate patterns. The decision whether or not to use a particular climate model to evaluate a certain impact should take into account explicitly the capability of that model to simulate a consistent spatial parameter of the mentioned impact. In this case, Q_{annual} or V—parameters obtained with low computational effort, could be employed as an additional tool to check the use of RCMs and GCMs to assess coastal dynamics. For example, this study's results suggest that RCM-GCM combination associated with HIR_E is not valid to evaluate LST processes.

Acknowledgements This research has been partly carried out during the visiting research stay of the first author in the Centre for Marine and Atmospheric Research, CSIRO (Commonwealth Scientific and Industrial Research Organisation) in the frame of her thesis work, which was funded by the *Ministerio de Educación* (Spanish Ministry of Education).

The authors gratefully acknowledge the research centres and institutions that freely and disinterestedly provided the atmospheric climate projections datasets used to assess the wave-driven impact on coastal sediment transport: *Danmarks Meteorologiske Institut*(DMI, Denmark) — special thanks to Ole B. Christensen, Neil Mackellar and Fredrik Boberg; *Koninklijk Nederlands Meteorologisch Instituut* (KNMI, The Netherlands) — special thanks to Erik van Meijgaard; *Insitut für Meterologie* (MPI, Germany) — special thanks to Daniela Jacob and Alberto Elizalde; *Sveriges Meteorologiska och Hydrologiska Institut* (SMHI, Sweden) — special thanks to Erik Kjellström and Barry Broman. We are also grateful to the *Organismo Público Puertos del Estado* (Spanish Ports and Harbors Authority) for providing HIPOCAS wave and atmospheric data.

References

Adams PN, Inman DL, Lovering JL (2011) Effects of climate change and wave direction on longshore sediment transport patterns in Southern California. Climatic Change 109(Suppl 1):S211–S228. DOI 10.1007/s10584-011-0317-0

Bayram A, Larson M, Hanson H (2007) A new formula for the total longshore sediment transport rate. Coastal Engineering 54:700–710. DOI 10.1016/j.coastaleng.2007.04.001

Bolaños-Sanchez R, Sánchez-Arcilla A, Cateura J (2007) Evaluation of two atmospheric models for wind-wave modelling in the NW Mediterranean. Journal of Marine Systems 65(1-4):336–353. DOI 10.1016/j.jmarsys.2005.09.014

Booij N, Ris RC, Holthuijsen LH (1999) A third-generation wave model for coastal regions 1. Model description and validation. Journal of Geophysical Research 104(C4):7649–7666. DOI 10.1029/98JC02622

Bosom E, Jiménez JA (2011) Probabilistic coastal vulnerability assessment to storms at regional scale — aplications to Catalan beaches (NW Mediterranean). Natural Hazards and Earth Systems Sciences 11:475–484. DOI 10.5194/nhess-11-475-2011

Callaghan DP, Ranasinghe R, Roelvink D (2013) Probablistic estimation of storm erosion using analytical, semi-empirical, and process based erosion models. Coastal Engineering 82:64–75. DOI 10.1016/j.coastaleng.2013.08.007

Casas-Prat M, Sierra JP (2012) Trend analysis of wave direction and associated impacts on the Catalan coast. Climatic Change 115(3):667–691. DOI 10.1007/s10584-012-0466-9

Casas-Prat M, Sierra JP (2013) Projected future wave climate in the NW Mediterranean Sea. Journal of Geophysical Research: Oceans 118(7):3548–3568. DOI 10.1002/jgrc.20233

Charles E (2012) Impact du changement climatique sur le climat de vagues en zone côtière, par régionalisation dynamique: application à la côte aquitane (in french). PhD thesis, Université de Toulose, 184 p

Christensen J H, Hewitson B, Busuioc A, Chen A, Gao X, Held I, Jones R, Kolli RK,Kwon W-T, Laprise R, Magaña Rueda V, Mearns L, Menéndez C G, Räisänen J, Rinke A, Sarr A, Whetton P (2007) Regional Climate Projections. In: Climate Change 2007: The Physical Science Basis. Contribution of Working Group I to the Fourth Assessment Report of the Intergovernmental Panel on Climate Change [Solomon, S., D. Qin, M. Manning, Z. Chen, M. Marquis, K.B. Averyt, M. Tignor and H.L. Miller (eds.)]. Cambridge University Press, Cambridge, United Kingdom and New York, NY, USA.

CIIRC (2010) Estat de la zona costanera a Catalunya (in Catalan). International Centre for Coastal Resources Research. Tech. rep., Barcelona

Coelho C, Silva R, Veloso-Gomes F, Taveira-Pinto F (2009) Potential effects of climate change on northwest Portuguese coastal zones. Journal of Marine Science 66:1497–1507. DOI 10.1093/icesjms/fsp132

Dickson ME, Walkden MJA, Hall JW (2009) Systemic impacts of climate change on an eroding coastal region over the twenty-first century. Climatic Change 84:141–166. DOI 10.1007/s10584-006-9200-9

Guedes Soares C, Weisse R, Carretero JC, Alvarez E (2002) A 40 years hindcast of wind, sea level and waves in European waters. In: Proceedings of OMAE 2002: 21st International Conference on Offshore Mechanics and Arctic Engineering, Oslo, Norway, June, pp 669–675

He X, Wang YP, and Zhu Q, Zhang Y, Zhang D, Zhang J, Yang Y, Gao J(2015) Simulation of sedimentary dynamics in a small-scale estuary: the role of human activities. Environmental Earth Sience 74:869–878. DOI 10.1007/s12665-015-4100-9

Hemer M, Fan Y, Mori N, Semedo A, Wang XL (2013) Projected change in wave climate from a multi-model ensemble. Nature Climate Change 3:471–476. DOI 10.1038/nclimate1791

Hemer MA (2009) Identifying coasts susceptible to wave climate change. Journal of Coastal Research SI 56:228–232

IPCC (2007) Special report. Emissions scenarios. Tech. rep.

Jiménez JA, Madsen OS (2003) A simple formula to estimate settling velocity of natural sediments. Journal of Waterway, Port, Coastal and Ocean Engineering(ASCE) 129:70–78. DOI 10.1016/S1674-2370(15)30017-X

Jiménez JA, Sancho-García A, Bosom E, Valdemoro HI, Guillén J (2012) Storm-induced damages along the Catalan coast (NW Mediterranean) during the period 1958-2008. Geomorphology 143–144:24–33. DOI 10.1016/j.geomorph.2011.07.034

Kalnay E, Kanamitsu M, Kistler R, Collins W, Deaven D, Gandin L, Iredell M, Saha S, White G, Woollen J, Zhu Y, Chelliah M, Ebisuzaki W, Higgins W, Janowiak J, Mo KC, Ropelewski C, Wang J, Leetmaa A, Reynolds R, Jenne R, Joseph D (1996) The NCEP/NCAR 40-year reanalysis project. Bulletin of the American Meteorological Society 77(3):437–471. DOI http://dx.doi.org/10.1175/1520-0477(1996)077⟨0437:TNYRP⟩2.0.CO;2

Kjellström E, Nikulin G, Hansson U, Strandberg G, Ullerstig A (2011) 21st century changes in the European climate: uncertainties derived from an ensemble of regional climate model simulations. Tellus A 63(1):24–40. DOI

10.1111/j.1600-0870.2010.00475.x
Larson M, Kraus N (1989) SBEACH: Numerical Model for Simulating Storm-Induced Beach Change, CERC-89-9, US Army Corps of Engineers. Tech. rep., Vicksburg
Leont'yev IO (2014) Calculation of Longshore Sediment Transport. Oceanology 54(2):205–211. DOI 10.1134/S0001437014020131
Mendoza ET, Jiménez JA (2006) Storm-induced beach erosion potential on the Catalonian coast. Journal of Coastal Research SI48:81–88
Mil-Homens J, Ranasinghe R, van Thiel de Vries JSM, Stive MJF (2013) Re-evaluation of the three commonly used bulk longshore sediment transport formulas. Coastal Engineering 75:29–39. DOI 10.1016/j.coastaleng.2013.01.004
Monbaliu J (2000) The spectral wave model, WAM, adapted for applications with high spatial resolution. Coastal Engineering 41(1-3):41–62. DOI 10.1016/S0378-3839(00)00026-0
Nicholls RJ, Kebede AS (2012) Indirect impacts of coastal climate change and sea-level-rise: the UK example. Climate Policy 12(sup01):S28–S52. DOI 10.1080/14693062.2012.728792
Pallarès E, Sánchez-Arcilla A, Espino M (2014) Wave energy balance in wave models (SWAN) for semi-enclosed domains–Application to the Catalan coast. Continental Shelf Research 87: 41–53 DOI 10.1016/j.csr.2014.03.008
Ratsimandresy AW, Sotillo MG, Alvarez-Fanjul E, Carretero-Albiach J, Perez-Gomez B, Hajji H (2008) A 44-year (1958–2001) sea level residual hindcast over the Mediterranean Basin. Physics and Chemistry of the Earth 33:250–259. DOI 10.1016/j.pce.2007.02.002
Sánchez-Arcilla A, Mösso C, Sierra JP, Mestres M, Harzallah A, Senouci M, El Raey M (2011) Climatic drivers of potential hazards in Mediterranean coasts. Regional Environmental Change 11(3):617–636. DOI 10.1007/s10113-010-0193-6
van Rijn LC, Walstra DJ, Grasmeijer B, Sutherland J, Pan S, Sierra JP (2003) The predictability of cross-shore bed evolution of sandy beaches at the time scale of storms and seasons using process-based profile models. Coastal Engineering 47:295–327. DOI 10.1016/S0378-3839(02)00120-5
Vericat D, Batalla RJ AD(2006) Sediment transport in a large impounded area: the lower Ebro, NE Iberian Peninsula. Geomorphology 79:71–92. DOI 10.1016/j.geomorph.2005.09.017
Villaret C, Hervowet JM, Kopmann R, Merkel U, Davies AG (2013) Morphodynamic modeling using the TELEMAC finite-element system. Computers & Geosciences 53:105–113. DOI 10.1016/j.cageo.2011.10.004
Wu XZ, Dong P(2015) Liouville equation-based stochastic model for shoreline evolution. Stochastic Environmental Research and Risk Assessment 7:1867–1880. DOI 10.1007/s00477-015-1029-1
Zacharioudaki A, Reeve DE (2011) Shoreline evolution under climate change wave scenarios. Climatic Change 108:73–105. DOI 10.1007/s10584-010-0011-7